Astron. & Astrophys. 40, 75—80 (1975)

Numerical Solution of Radiative Transfer Equation in Extended Spherical Atmospheres with Rayleigh Phase Function

A. Peraiah
Lehrstuhl für Theoretische Astrophysik der Universität, Heidelberg

Received January 15, revised March 7, 1975

Summary. A numerical solution of radiative transfer equation has been obtained in spherically symmetric homogeneous medium with Rayleigh's phase function in the frame work of discrete space theory of Grant and Hunt (1968) and Peraiah and Grant (1973). The fast doubling algorithm has been used in spherical cases for large optical thicknesses and highly extended spherical shells. Fluxes have been conserved to the machine accuracy except in the case of large values of B/A (ratio of outer to inner radius of the atmosphere) where doubling algorithm has been used and flux is conserved up to few units in the sixth decimal place. The linear polarization is found to be about 15% for $B/A = 5$ and $\tau = 5$–10 (where τ is the total optical depth of the medium).

Key words: radiative transfer-spherical atmospheres-Rayleigh phase function

1. Introduction

Chandrasekhar (1950) gave an explicit mathematical formulation for the equation of transfer of linearly polarized radiation in plane parallel atmospheres. Further work on this problem was done by Code (1950), Harrington (1969, 1970) and others all of whom assumed plane parallel approximation.

The quasi-stellar object 3C446 showed a high degree of polarization (Burbidge and Burbidge, 1967, p. 77) of about 10%. In estimating fluxes from a "standard" QSO, they found (p. 121) that the radius of the shell to be about 10^{19} cm with a thickness of 10^{17} cm which suggests the presence of extended atmospheres attached to these objects (although the atmosphere is not highly extended, the presence of scattering complicates the calculation of the solution of radiative transfer equation). Recently Serkowski (1970) found polarization in the stars with extended atmospheres or spherical shells. Polarization has also been found in late type stars (Vardya, 1970 and see references given there). Polarization is caused by scattering by electrons in early type stars and by molecules in late type stars and both types of scatterings have the same angular distribution given by the solution of transfer equation with Rayleigh's phase function. Consequently one must take scattering into account in calculating the transfer of linearly polarized radiation. Whenever there is scattering in transfering radiation, we may have to iterate for the solution of the transfer equation. In problems dealing with spherical symmetry, the ray continuously changes its direction with the radius vector which amounts again to some sort of scattering, which we shall call curvature-scattering. This, taken together with the scattering either by electrons or by molecules would greatly complicate the process of emergence of radiation from such atmospheres. There have been some attempts towards these problems in the recent past (Cassinelli and Hummer, 1971; Schmidt-Burgk, 1973, and others). Peraiah and Grant (1973, henceforth called paper I) developed a method to calculate a direct numerical solution of radiative transfer equation in spherical shells based on the discrete space theory of Grant and Hunt (1969a, b). A slightly different version of this approach was used by Plass *et al.* (1973) and was found to be an extremely fast algorithm by which one can calculate the radiation field at any given point inside the medium directly.

We shall calculate the angular distribution of linear polarization in extended homogeneous spherical medium with Rayleigh's phase function. The primary aim of this paper is just to see how curvature affects the emergent radiation field from a completely scattering medium. However, one cannot compare these results with those of observations as one observes fluxes from either a distorted surface of a star or from one of the components of a close binary system during eclipse where as we calculate mainly the angular distribution of the specific intensities. The polarization of distorted stars with extended atmospheres will be treated in a forthcoming paper.

2. Discretization of Radiative Transfer Equation

The transfer equation in divergence form in spherical symmetry is

$$\frac{\mu}{r^2}\frac{\partial}{\partial r}\{r^2 I(r,\mu)\}+\frac{1}{r}\frac{\partial}{\partial \mu}\{(1-\mu^2)I(r,\mu)\}+\sigma(r)I(r,\mu)$$

$$=\sigma(r)\left\{[1-\varpi(r)]b(r)+\frac{\varpi(r)}{2}\int_{-1}^{+1}P(r,\mu,\mu')I(r,\mu')\,d\mu'\right\}, \quad (1)$$

where $\varpi(r)$ is the albedo for single scattering, $I(r,\mu)$ is the specific intensity, $r=$ radius, $\mu=\cos\theta$, $\sigma(r)$ is the absorption coefficient, $b(r)$ is the source inside the medium and $p(r,\mu,\mu')$ is the phase function.
If we write

$$U(r,\mu)=r^2 I(r,\mu) \quad (2)$$

and set $\varpi(r)=1$, (as we are considering only scattering) we can rewrite Eq. (1) as,

$$\mu\frac{\partial U(r,\mu)}{\partial r}+\frac{1}{r}\frac{\partial}{\partial\mu}\{(1-\mu^2)U(r,\mu)\}+\sigma(r)U(r,\mu)$$

$$=\frac{\sigma(r)}{2}\int_{-1}^{+1}P(r,\mu,\mu')U(r,\mu')\,d\mu' \quad (3)$$

for positive $\mu\in(0,1)$.
And

$$-\mu\frac{\partial U(r,-\mu)}{\partial r}-\frac{1}{r}\frac{\partial}{\partial\mu}\{(1-\mu^2)U(r,-\mu)\}+\sigma(r)U(r,-\mu)$$

$$=\frac{\sigma(r)}{2}\int_{-1}^{+1}P(r,-\mu,\mu')\,U(r,\mu')\,d\mu' \quad (4)$$

for the oppositely directed beam.
If the radiation field is represented by two perpendicularly polarized intensity beams, then

$$U(r,\mu)=\begin{bmatrix}U_L(r,\mu)\\U_R(r,\mu)\end{bmatrix}, \quad (5)$$

where U_L and U_R refer respectively to the states of polarization in which the electric vector vibrates along and perpendicular to the principle meridian. The phase function is given by (see Grant and Hunt, 1968),

$$P(r,\mu,\mu')=\tfrac{3}{4}\begin{bmatrix}2(1-\mu^2)(1-\mu'^2) & \mu^2\\ \mu'^2 & 1\end{bmatrix}$$

$$=\begin{bmatrix}P_{11}(\mu,\mu') & P_{12}(\mu,\mu')\\ P_{21}(\mu,\mu') & P_{22}(\mu,\mu')\end{bmatrix}. \quad (6)$$

Now the transfer equation for each component U_L and U_R can be written as,

$$\mu\frac{\partial U_L(r,\mu)}{\partial r}+\frac{1}{r}\frac{\partial}{\partial\mu}\{(1-\mu^2)U_L(r,\mu)\}+\sigma(r)U_L(r,\mu)$$

$$=\frac{\sigma(r)}{2}\int_{-1}^{+1}[P_{11}(\mu,\mu')U_L(r,\mu')+P_{12}(\mu,\mu')U_R(r,\mu')]\,d\mu' \quad (7)$$

and

$$-\mu\frac{\partial U_L(r,-\mu)}{\partial r}-\frac{1}{r}\frac{\partial}{\partial\mu}\{(1-\mu^2)U_L(r,-\mu)\}$$

$$+\sigma(r)U_L(r,-\mu)$$

$$=\frac{\sigma(r)}{2}\int_{-1}^{+1}[P(-\mu,\mu')U_L(r,\mu')$$

$$+P_{12}(-\mu,\mu')U_R(r,\mu')]\,d\mu'. \quad (8)$$

The equations for U_R are similar.
The discrete representation of Eqs. (7) and (8) together with the two similar equations for U_R is written following paper I as,

$$\boldsymbol{M}^*[\boldsymbol{U}^+_{n+1}-\boldsymbol{U}^+_n]+\varrho_c[\boldsymbol{\Lambda}^*_+\boldsymbol{U}^-_{n+\frac12}+\boldsymbol{\Lambda}^*_-\boldsymbol{U}^-_{n+\frac12}]+\tau_{n+\frac12}\boldsymbol{U}^+_{n+\frac12}$$

$$=\tfrac12\tau_{n+\frac12}\{\boldsymbol{P}^{++}_{n+\frac12}\boldsymbol{c}^*\boldsymbol{U}^+_{n+\frac12}+\boldsymbol{P}^{+-}_{n+\frac12}\boldsymbol{c}^*\boldsymbol{U}^-_{n+\frac12}\} \quad (9)$$

and

$$\boldsymbol{M}^*[\boldsymbol{U}^-_n-\boldsymbol{U}^-_{n+1}]-\varrho_c[\boldsymbol{\Lambda}^*_+\boldsymbol{U}^-_{n+\frac12}+\boldsymbol{\Lambda}^*_-\boldsymbol{U}^+_{n+\frac12}]+\tau_{n+\frac12}\boldsymbol{U}^-_{n+\frac12}$$

$$=\tfrac12\tau_{n+\frac12}\{\boldsymbol{P}^{-+}_{n+\frac12}\boldsymbol{c}^*\boldsymbol{U}^+_{n+\frac12}+\boldsymbol{P}^{--}_{n+\frac12}\boldsymbol{c}^*\boldsymbol{U}^-_{n+\frac12}\}, \quad (10)$$

where

$$\boldsymbol{U}^\pm_n=\begin{bmatrix}\boldsymbol{U}^\pm_n(L)\\ \boldsymbol{U}^\pm_n(R)\end{bmatrix}$$

$$\boldsymbol{U}^+_n(L)=\begin{bmatrix}U_{n,1}(L)\\U_{n,2}(L)\\\vdots\\U_{n,m}(L)\end{bmatrix} \text{ and } \boldsymbol{U}^-_n(L)=\begin{bmatrix}U_{n,-1}(L)\\U_{n,-2}(L)\\\vdots\\U_{n,-m}(L)\end{bmatrix}, \quad (11)$$

$$U_{n,\pm j}(L)=U_L(r_n,\pm\mu_j), \quad j=1,2,\ldots,m.$$

The vector $\boldsymbol{U}^\pm_n(R)$ is similarly defined. And,

$$\boldsymbol{M}^*=\begin{bmatrix}\boldsymbol{M} & \cdot\\ \cdot & \boldsymbol{M}\end{bmatrix}, \quad \boldsymbol{M}=[\mu_j\delta_{jk}]; \quad \boldsymbol{c}^*=\begin{bmatrix}\boldsymbol{c} & \cdot\\ \cdot & \boldsymbol{c}\end{bmatrix},$$

$$\boldsymbol{c}=[c_j\delta_{jk}]$$

$$j,k=1,2,\ldots,m,$$

where μ_j's and c_j's are the roots and weights of a suitable quadrature formula. Furthermore,

$$\boldsymbol{P}^{++}_{\alpha\beta}|_{n+\frac12}=\boldsymbol{P}_{\alpha\beta}(+\mu_j,+\mu_k)=\boldsymbol{P}^{--}_{\alpha\beta}|_{n+\frac12}$$

$$\boldsymbol{P}^{+-}_{\alpha\beta}|_{n+\frac12}=\boldsymbol{P}_{\alpha\beta}(\mu_j,-\mu_k)=\boldsymbol{P}^{-+}_{\alpha\beta}|_{n+\frac12}$$

$$\alpha,\beta=1,2; \quad \mu_j,\mu_k>0,$$

and

$$\boldsymbol{P}^{++}_{n+\frac12}=\begin{bmatrix}\boldsymbol{P}^{++}_{11} & \boldsymbol{P}^{++}_{12}\\ \boldsymbol{P}^{++}_{21} & \boldsymbol{P}^{++}_{22}\end{bmatrix}$$

with similar expressions for $\boldsymbol{P}^{-+}_{n+\frac12}, \boldsymbol{P}^{+-}_{n+\frac12}, \boldsymbol{P}^{--}_{n+\frac12}$; $n+\frac12$ represents the average of the cell bounded by r_n and r_{n+1}.
[A cell is defined as that which has it's thickness less than or equal to the critical step size. See Eq. (18).] And,

$$\tau_{n+\frac12}=\int_{r_{n+1}}^{r_n}\sigma(r)\,dr=\sigma_{n+\frac12}(r_n-r_{n+1}).$$

The curvature factor ϱ_c is defined as

$$\varrho_c = \Delta r/\bar{r},$$

where Δr is the thickness of the cell (geometrical) and $\bar{r}$ is the mean radius of the cell. In all these calculations we have taken $\bar{r}$ as the outer radius of the basic cell. And,

$$\Lambda^*_{\pm} = \begin{bmatrix} \Lambda_{\pm} & \cdot \\ \cdot & \Lambda_{\pm} \end{bmatrix},$$

where $\Lambda_{\pm}$ are curvature matrices (see paper I or Peraiah, 1973). The average intensities over the cell are expressed as a weighted mean of the interface intensities. Thus,

$$(\boldsymbol{I} - \boldsymbol{X}^{+}_{n+\frac{1}{2}})\boldsymbol{U}^{+}_{n} + \boldsymbol{X}^{+}_{n+\frac{1}{2}}\boldsymbol{U}^{+}_{n+1} = \boldsymbol{U}^{+}_{n+\frac{1}{2}}, \tag{12}$$

$$(\boldsymbol{I} - \boldsymbol{X}^{-}_{n+\frac{1}{2}})\boldsymbol{U}^{-}_{n+1} + \boldsymbol{X}^{-}_{n+\frac{1}{2}}\boldsymbol{U}^{-}_{n} = \boldsymbol{U}^{-}_{n+\frac{1}{2}}, \tag{13}$$

where $\boldsymbol{X}^{\pm}_{n+\frac{1}{2}}$ are $2m \times 2m$ diagonal matrices with the structure

$$\boldsymbol{X}^{\pm}_{n+\frac{1}{2}} = \begin{bmatrix} \boldsymbol{X}_{n+\frac{1}{2}}(L) & \cdot \\ \cdot & \boldsymbol{X}_{n+\frac{1}{2}}(R) \end{bmatrix} \tag{14}$$

where $\boldsymbol{X}_{n+\frac{1}{2}}$ are diagonal $m \times m$ matrices. Usually, we choose $\boldsymbol{X}_{n+\frac{1}{2}} = \frac{1}{2}\boldsymbol{I}$ ($\boldsymbol{I}$ is the identity matrix) for diamond scheme and $\boldsymbol{X}_{n+\frac{1}{2}} = \boldsymbol{I}$ for "step" scheme (Carlson, 1963). Other choices of intermediate character are available (Grant, 1968).

It is now straight-forward to calculate the transmission and reflection matrices for a given shell of thickness τ from Eqs. (9) and (10) following paper I [see Eqs. (2.13) and (2.14) and the Appendix].

Flux conservation is ensured by satisfying the necessary condition [see the last of Eq. (3.6) of paper I] that

$$\|S(n, n+1)\| = 1$$

which, in terms of transmission and reflection matrices (see Appendix of paper I) becomes,

$$\begin{aligned} &\|T(n+1, n) + R(n+1, n)\| = 1 \\ &\|T(n, n+1) + R(n, n+1)\| = 1\,. \end{aligned} \tag{15}$$

And this leads to the two relations [Eq. (4.3) of paper I]

$$(1)\ \sum_{j=1}^{m} c_j(\Lambda^{+}_{jk} - \Lambda^{-}_{jk}) = 0 \quad \text{for all } k \tag{16}$$

and [from Eq. (3.9) of Grant and Hunt, 1969b]

$$\begin{aligned} (2)\ \tfrac{1}{2}\sum_{j=1}^{m} c_j[&P_{11}(\mu_j, \mu_k) + P_{21}(\mu_j, \mu_k) \\ &+ P_{11}(-\mu_j, \mu_k) + P_{21}(-\mu_j, \mu_k)] = 1 \quad \text{for all } k, \end{aligned} \tag{17}$$

and

$$\begin{aligned} \tfrac{1}{2}\sum_{j=1}^{m} c_j[&P_{21}(\mu_j, \mu_k) + P_{22}(\mu_j, \mu_k) + P_{12}(-\mu_j, \mu_k) \\ &+ P_{22}(-\mu_j, \mu_k)] = 1 \quad \text{for all } k\,, \end{aligned}$$

and two other similar equations for $P^{--}_{n+\frac{1}{2}}$ and $P^{+-}_{n+\frac{1}{2}}$.

The right hand side of Eq. (17) need not be exactly 1 because the calculation of the p matrices depend upon μ'^{s}_{j} which are taken from any quadrature formula depending upon the requirement of the problem. If this is not satisfied exactly, renormalization of the elements of these matrices is necessary (see Plass *et al.*, 1973). We have used the zeroes and weights of Gauss-Legendre quadrature on [0, 1] and the relations (17) are satisfied to the machine accuracy.

The emergent radiation field can be calculated either by the internal field algorithm or by the external field algorithm (Grant and Hunt, 1968). The former calculates the radiation field at any point inside the medium at the expense of large machine storage space and the latter calculates only the emergent radiation without any need of storage space, to the same accuracy. We have used both algorithms depending upon the result that is sought.

3. Results and Discussion

Calculations have been made for optical depths up to 10 and the ratio B/A (ratio of outer to inner radius of the spherical medium) has been taken from 1 to 5. Fifty discrete points along the radial direction are choosen ($N = 50$). The step size $\Delta\tau$ is choosen so that

$$\Delta\tau < \Delta\tau_{\text{crit}} = \min_j \left| \frac{\mu_j \pm \frac{1}{2}\varrho\Lambda^{+}_{jj}}{\frac{1}{2}(1 - \varpi p^{++}_{jj} c_j)} \right| \tag{18}$$

to ensure non-negativity and hence stability of the algorithm. The curvature factor of the outermost shell is

$$\varrho_{\text{out}} = \frac{B - A}{NB} \tag{19}$$

and in terms of ϱ_{out} we can calculate ϱ_n for any shell n as

$$\varrho_n = \frac{\varrho_{\text{out}}}{1 - (n-1)\varrho_{\text{out}}}. \tag{20}$$

To maintain stability and non-negativity of the solution, we must obtain non-negative transmission and reflection matrices (for simplicity we write t and r matrices) which satisfy the relation (15) [see Section (3) of paper I] and their calculation involves the stepsize restriction given by the inequality (18) containing the curvature factor ϱ as defined in (19) and (20). This forces us to select small ϱ's in consequence of which we have to employ a large number of shells. Therefore we have to use a proportionately large machine storage space as the diffuse transmission and reflection matrices are to be stored at the boundary of each shell.

We divide the medium of interest into N shells (where N depends mostly on the machine capacity) and if in any shell, $\Delta\tau > \Delta\tau_{\text{crit}}$ then subdivide it into smaller shells until, in each shell the condition $\Delta\tau < \Delta\tau_{\text{crit}}$ is satisfied. Now, the t & r matrices for each subshell with its ϱ are

calculated and they are added by star algorithm [see Eqs. (3.7) and (3.8), paper I] to obtain the t & r matrices for the original shell. However, from Eqs. (19) and (20), we see that ϱ increases from the surface ($n=1$) to the bottom ($n=N$) of the atmosphere and hence the number of subshells in each shell increases and so does the number of star additions—a time consuming process. So, instead of calculating the t & r matrices for each of the subshells with different ϱ's, we can calculate them by using an average ϱ of all subshells and add them by star product, doubling the shells everytime we use the star algorithm which we shall call doubling process. By this process, we can save about 50% on the computing time but with some loss of accuracy. The flux could be conserved up to few units in the sixth decimal place. The system seems to be quite stable even when we use quite large optical thicknesses and highly extended spherical shells.

After we calculate the t & r matrices, the radiation field can be computed by means of either internal field or external field algorithms with the boundary conditions given below.

No incident radiation has been given at $T=0(n=1)$.

$$U_1^+(L)=0 \qquad U_1^+(R)=0 \qquad \text{for all } \mu_j$$

and an unpolarized radiation is incident at $\tau=T(n=N+1)$

$$U_{N+1}^-(L)=1 \qquad U_{N+1}^-(R)=1 \qquad \text{for all } \mu_j$$

so that the flux $\sum_{j=1}^{m} U_{N+1}^-(L \text{ or } R)\mu_j c_j = 1$.

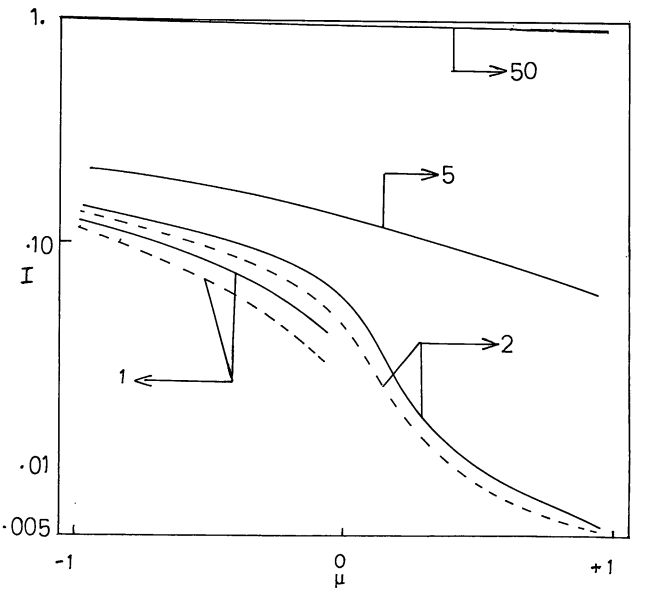

Fig. 1. The angular distribution of specific intensities ($I_L=U_L/r^2$ and $I_R=U_R/r^2$) for the radial coordinate r_n ($n=1$ to 50) for $B/A=1$ and $\tau=10$. Dashed curves represent I_L and continuous curves represent I_R. Resolution between I_L and I_R can be found only from $n\leqq 5$. Numbers represent n

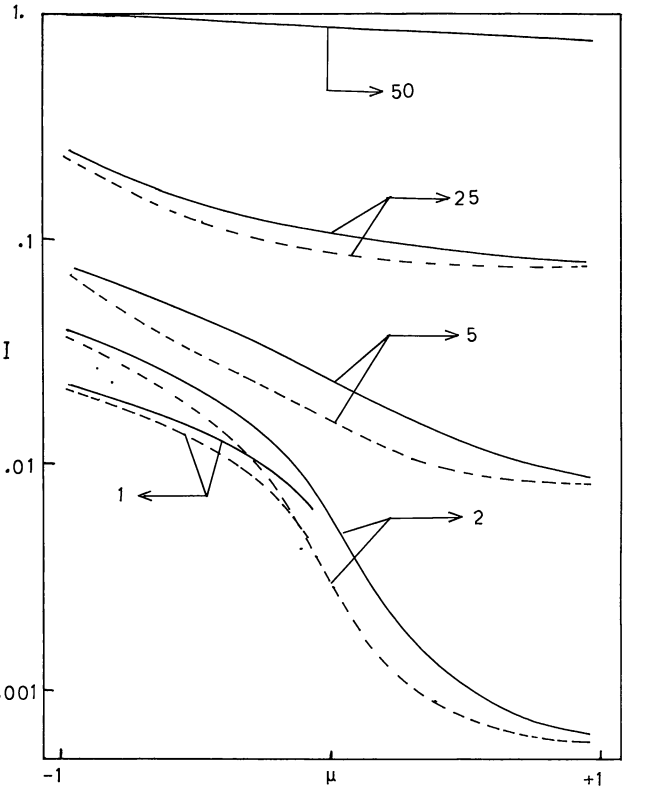

Fig. 2. Same as in Fig. 1 except that $B/A=5$, i.e., spherical case. Notice that I_L and I_R are resolved all along the radius except deep inside the medium. Notice also that at $\mu\approx+1$ or -1, $I_L=I_R$ which is true for $B/A=1$ in Fig. 1 also. Numbers refer to n

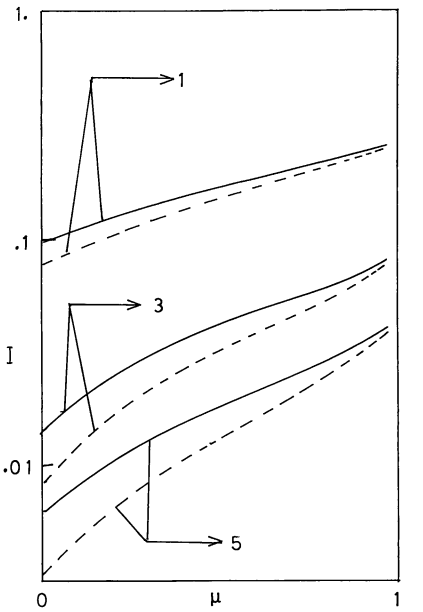

Fig. 3. Angular distribution of the emergent radiation for the indicated values of B/A. Dashed curves represent I_L and continuous curves represent I_R. Notice that at $\mu\approx 1$, $I_L=I_R$

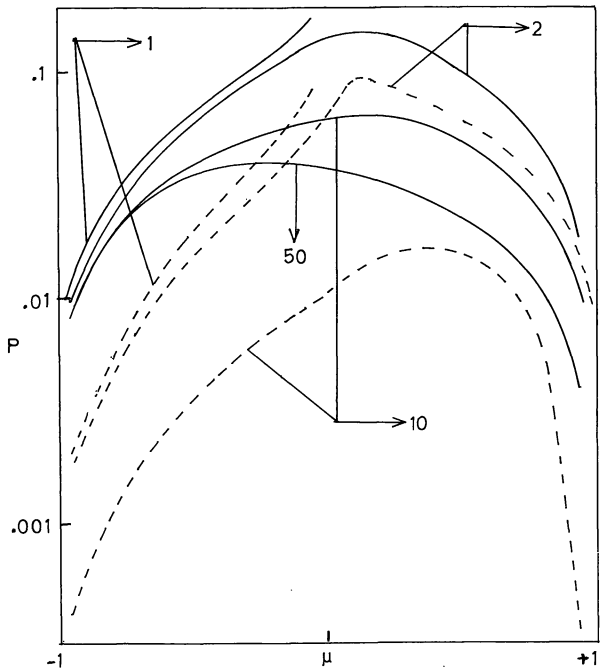

Fig. 4. The angular distribution of polarization along the radius vector ($n=1$ to 50) for $\tau=10$ is given. Continuous curves represent spherical case for $B/A=5$ and dashed curves represent plane parallel case for $B/A=1$. At $n=50$, for $B/A=1$ the polarization is too small to be shown here. Numbers refer to n

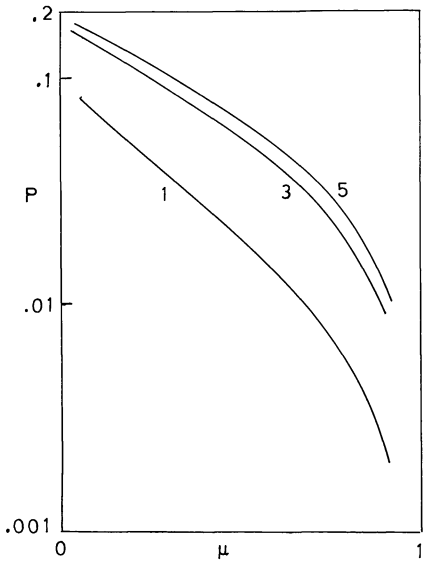

Fig. 5. Angular distribution of polarization of the emergent radiation for $\tau=10$ and for the indicated parameters of B/A (=1 to 5)

The degree of polarization P_n of radiation from any shell n is calculated by the relation

$$P_n^{\pm}=\frac{U_n^{\pm}(R)-U_n^{\pm}(L)}{U_n^{\pm}(R)+U_n^{\pm}(L)}. \qquad (21)$$

The results are presented in Figs. 1–6. In Figs. 1 and 2 we have shown the angular distribution of specific

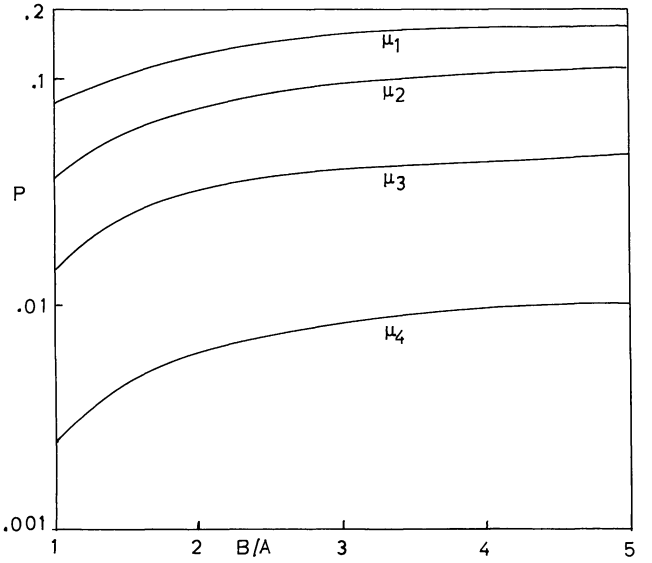

Fig. 6. Polarization is plotted for each angle $\mu_j(j=1$ to 4) ($\cos^{-1}\mu_1\approx 86°$, $\cos^{-1}\mu_2\approx 71°$, $\cos^{-1}\mu_3\approx 47°$, $\cos^{-1}\mu_4\approx 22°$) for $\tau=10$ against B/A

intensities I_R and $I_L(=(U_R, U_L)/r^2)$ along the radial direction for plane parallel and spherical cases respectively, for the indicated parameters of τ and B/A. One can notice that the differences between I_R and I_L are larger in spherical system than in plane parallel systems and hence larger polarization in the former systems. This is due to the fact that curvature scattering enhances the effects of Rayleigh's scattering. In Fig. 3 we have given the angular distribution of the emergent radiation for $B/A=1, 3, 5$ and $\tau=5$ which is quite similar in its nature of variation to that in Fig. 4 of paper I. We notice that the difference between I_L and I_R diminishes as we go from $\mu\approx 0$ to $\mu\approx 1$, that is, the polarization increases towards the limb. In Fig. 4 the radial distribution of polarization defined by Eq. (21) is plotted against $\mu\in[-1, +1]$. Here $n=50$ and $n=1$ correspond respectively to the bottom and surface of the atmosphere. One can notice that both in plane parallel and spherical cases there is a progressive increase in polarization towards the surface. In plane parallel case the polarization is less than that in spherical case at a given point in the atmosphere. However, the maximum of polarization occurs around $\mu\approx 0$ more towards into the atmosphere. This is more so in plane parallel than in spherical case. So, one should generally be able to observe polarization in stars with extended atmospheres which explains the fact that Serkowski (1970) found polarization only in the stars with extended shells or atmospheres. The emergent angular distribution of polarization given in Eq. (21) is plotted for $B/A=1, 3$ and 5 in Fig. 5. There is a substantial difference between polarization for $B/A=1$ and that for $B/A=3$ and a further increase in B/A from 3 to 5 does not significantly increase the polarization as fast as it was from that at $B/A=1$ to

that at $B/A = 3$. Figure 6 gives the trend of polarization with respect to B/A for each ray. Again, in spherical case we find more polarization than in plane parallel case. From these results we notice that the polarization could be as large as 15%. One must however investigate the polarization of radiation from the distorted surface of a star which is under consideration.

Acknowledgments. I wish to thank Dr. I. P. Grant of Pembroke College, Oxford, England, Professor G. Traving, Professor B. Baschek, Dr. J. Schmidt-Burgk and W. H. Kegel for helpful comments and criticism on the manuscript.
This work has been performed as part of the Sonderforschungsbereich 132 "Theoretische und praktische Stellarastronomie" which is sponsored by the Deutsche Forschungsgemeinschaft.

References

Burbidge, G., Burbidge, M. 1967, Quasi-Stellar Objects, W. H. Freeman and Company; San Francisco and London
Carlson, B. G. 1963, Methods of Computational Physics **1**, pp. 1—42, ed. by B. Adler, S. Fernbach and M. Rotenberg, Academic Press, New York
Cassinelli, J. P., Hummer, D. G. 1971, *Monthly Notices Roy. Astron. Soc.* **153**, 9
Chandrasekhar, S. 1950, Radiative Transfer, Oxford University Press
Code, A. D. 1950, *Astrophys. J.* **112**, 22
Grant, I. P. 1968, *J. Comp. Phys.* **2**, 281
Grant, I. P., Hunt, G. E. 1968, *J. Quant. Spectrosc. Radiat. Transfer.* **8**, 1817
Grant, I. P., Hunt, G. E. 1969a, *Proc. Roy. Soc. London* A, **313**, 183
Grant, I. P., Hunt, G. E. 1969b, *Proc. Roy. Soc. London* A, **313**, 199
Harrington, J. P. 1969, *Astrophys. J. Letters* **3**, 165
Peraiah, A. 1973, *Astrophys. Space Sci.* **21**, 223
Peraiah, A., Grant, I. P. 1973, *J. Inst. Maths. Appl.* **12**, 75 (Paper I)
Plass, G. N., Kattawar, G. W., Catchings, F. E. 1973, *Appl. Optics.* **12**, 314
Schmidt-Burgk, J. 1973, *Astrophys. J.* **181**, 865
Serkowski, K. 1970, *Astrophys. J.* **160**, 1083
Vardya, M. S. 1970, *Ann. Rev. Astron. Astrophys.* **8**, 87

A. Peraiah
Lehrstuhl für Theoretische Astrophysik
der Universität Heidelberg
D-6900 Heidelberg 1
Im Neuenheimer Feld 294
Federal Republic of Germany